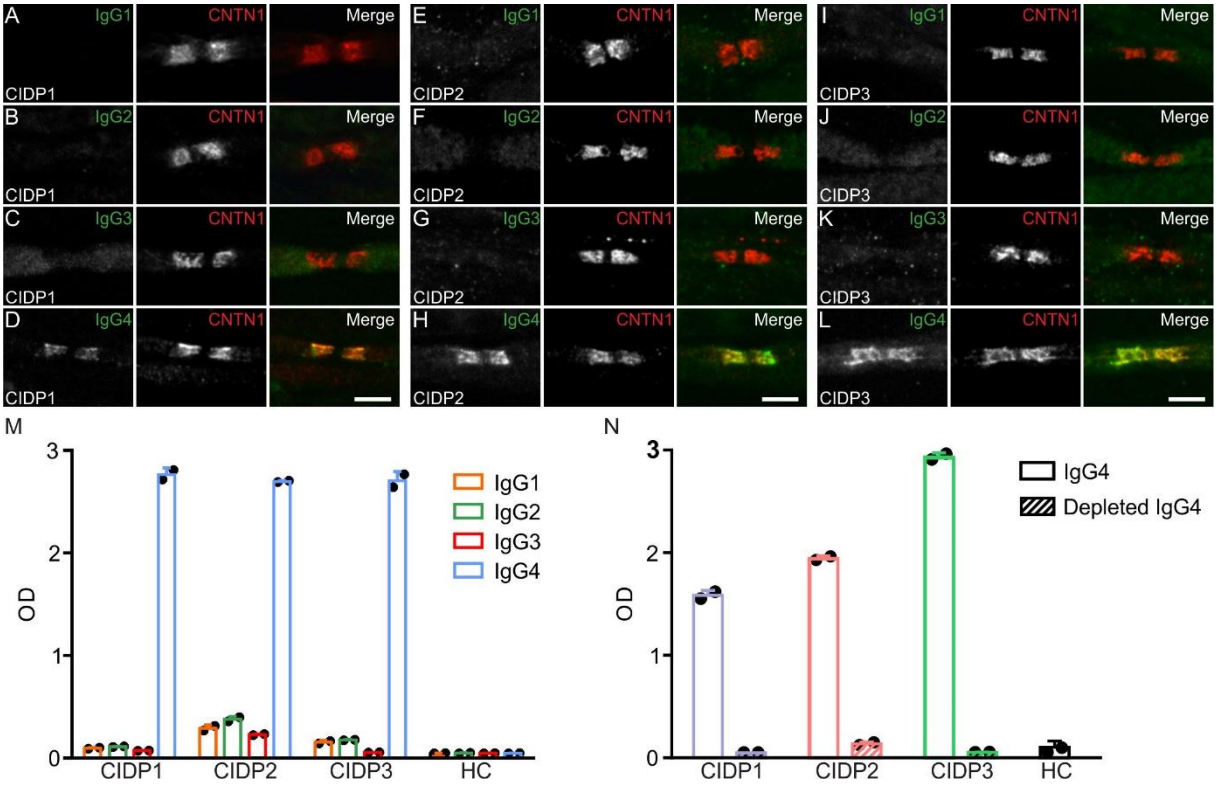

Supplemental Figure 1. Reactivity of IgG isotypes to human Nfasc155 and paranodes. (**A-L**) These are teased rat sciatic nerves immunostained for CNTN1 (red) and the plasma or serum samples from three CIDP patients (CIDP1-3) positive for anti-Nfasc155 IgG4 (1/200; green), then revealed with FITC conjugated mouse anti-human IgG1 (**A, E,** and **I**), IgG2 (**B, F,** and **J**), IgG3 (**C, G,** and **K**), or IgG4 (**D, H,** and **L**). The IgG4 from these samples presented a strong reactivity toward paranodes. (**M**) Reactivity of IgG isotypes against human Nfasc155 was examined by ELISA in the three CIDP patients and four healthy controls (HC). The three patients presented a predominant IgG4 reactivity against Nfasc155. (**N**) Purified IgG4 from three CIDP patients were incubated with human Nfasc155 conjugated to agarose beads in order to deplete those samples of anti-Nfasc155 autoantibodies. The IgG4 fractions were then tested by ELISA against human Nfasc155, as well as the IgG4 fraction without adsorption from a healthy control (HC). The incubation with Nfasc155-beads abolished the reactivity against Nfasc155 in all CIDP patients. Scale bar: 10 μm.

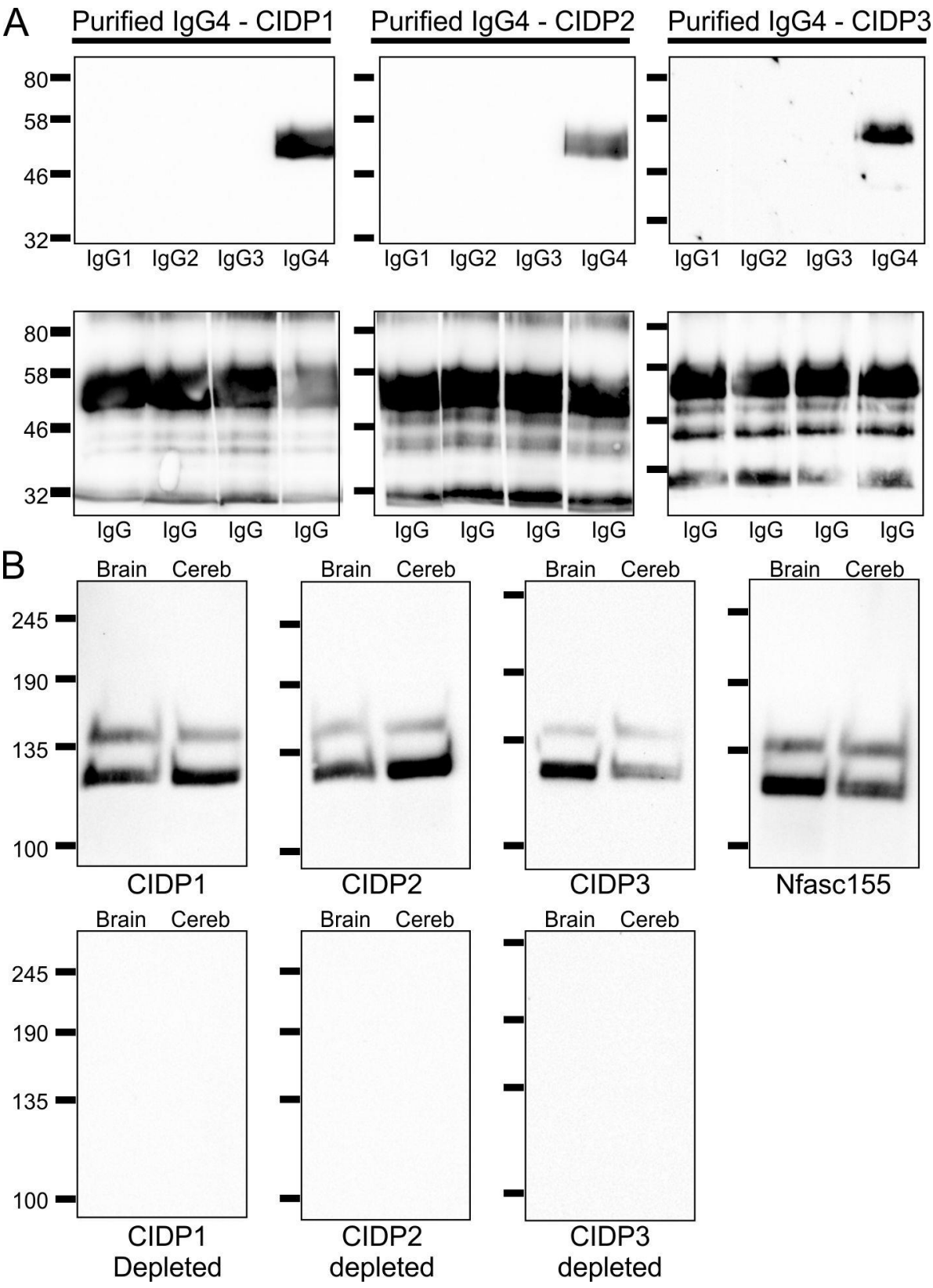

Supplemental Figure 2. Purification of anti-Nfasc155 IgG4.

(**A**) IgG4 from three CIDP patients (CIDP1-3) were purified using CaptureSelect™ affinity matrix. The purified IgG4 samples (1 μg) were loaded on SDS-PAGE gels and immunoblotted with IgG isotype specific antibodies (upper panels) or IgG specific antibodies (lower panels).

No contamination with the different IgG isotypes was observed. (**B**) Adult rat brain and cerebellum proteins (50 µg) were separated by western-blot and immunoblotted with purified IgG4 fractions from three CIDP patients (left panels) or a rabbit antibody against Nfasc155 (right panel). CIDP IgG4 reacted against the high and low isoforms of Nfasc155 in brain and cerebellum. The depletion of anti-Nfasc155 IgG4 abolished the reactivity against brain and cerebellum sample proteins. Molecular weight markers are indicated in kDa on the left.

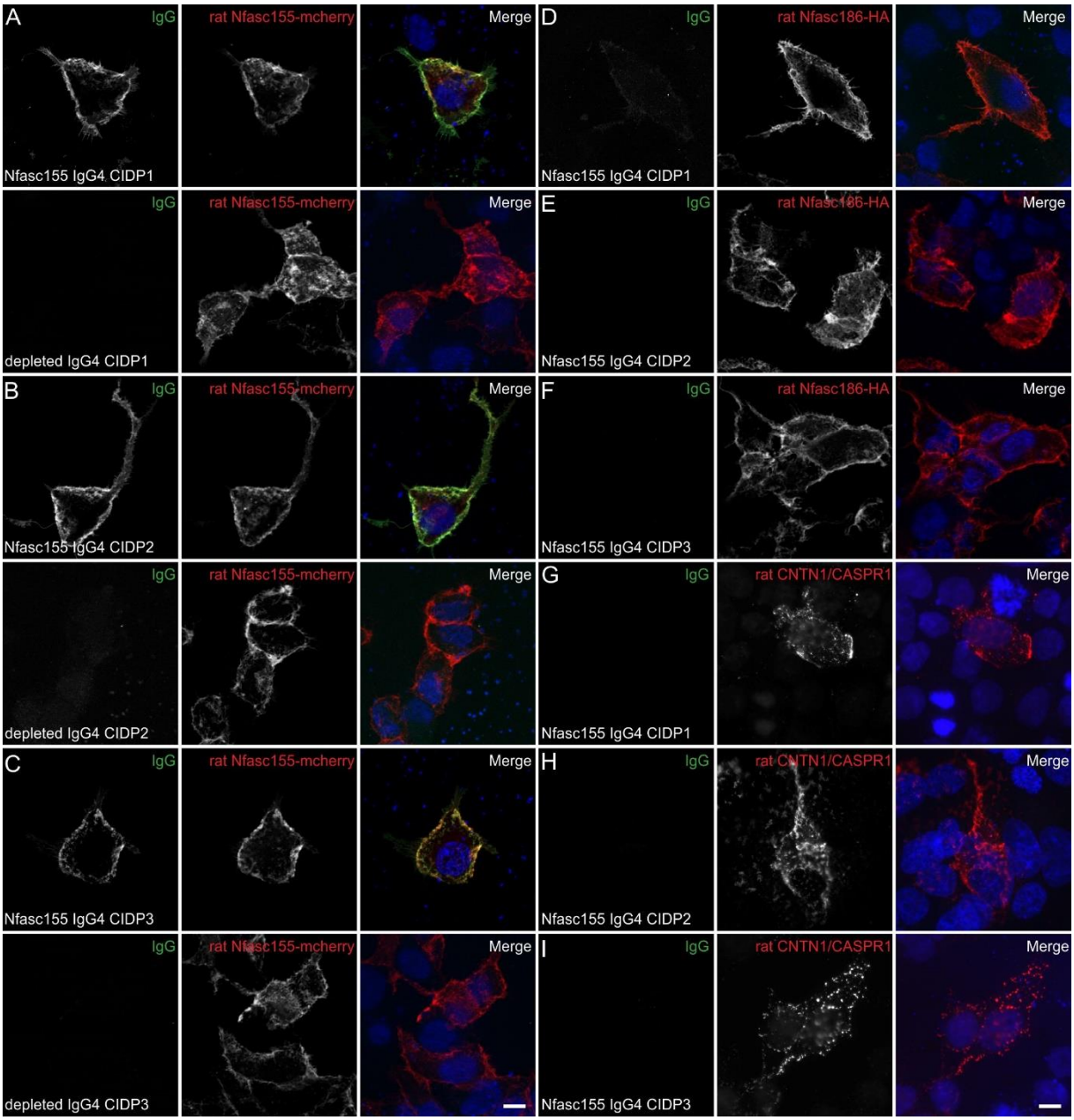

Supplemental Figure 3. Autoantibodies recognize rat Nfasc155, but not rat Nfasc186 or CNTN1/CASPR1.

(**A-I**) The purified IgG4 fractions from three CIDP patients (CIDP1-3) were tested on HEK cells transfected with rat mcherry-tagged Nfasc155, rat HA-tagged Nfasc186, or rat CNTN1/CASPR1 as indicated. The IgG4 fractions (green) from the three CIDP patients reacted against rat Nfasc155. By contrast, no samples recognized rat Nfasc186 or CNTN1/CASPR1. The immunoadsorption against Nfasc155-beads (depleted IgG4) abolished the reactivity against rat Nfasc155 in all CIDP patients. Scale bar: 10 μm.

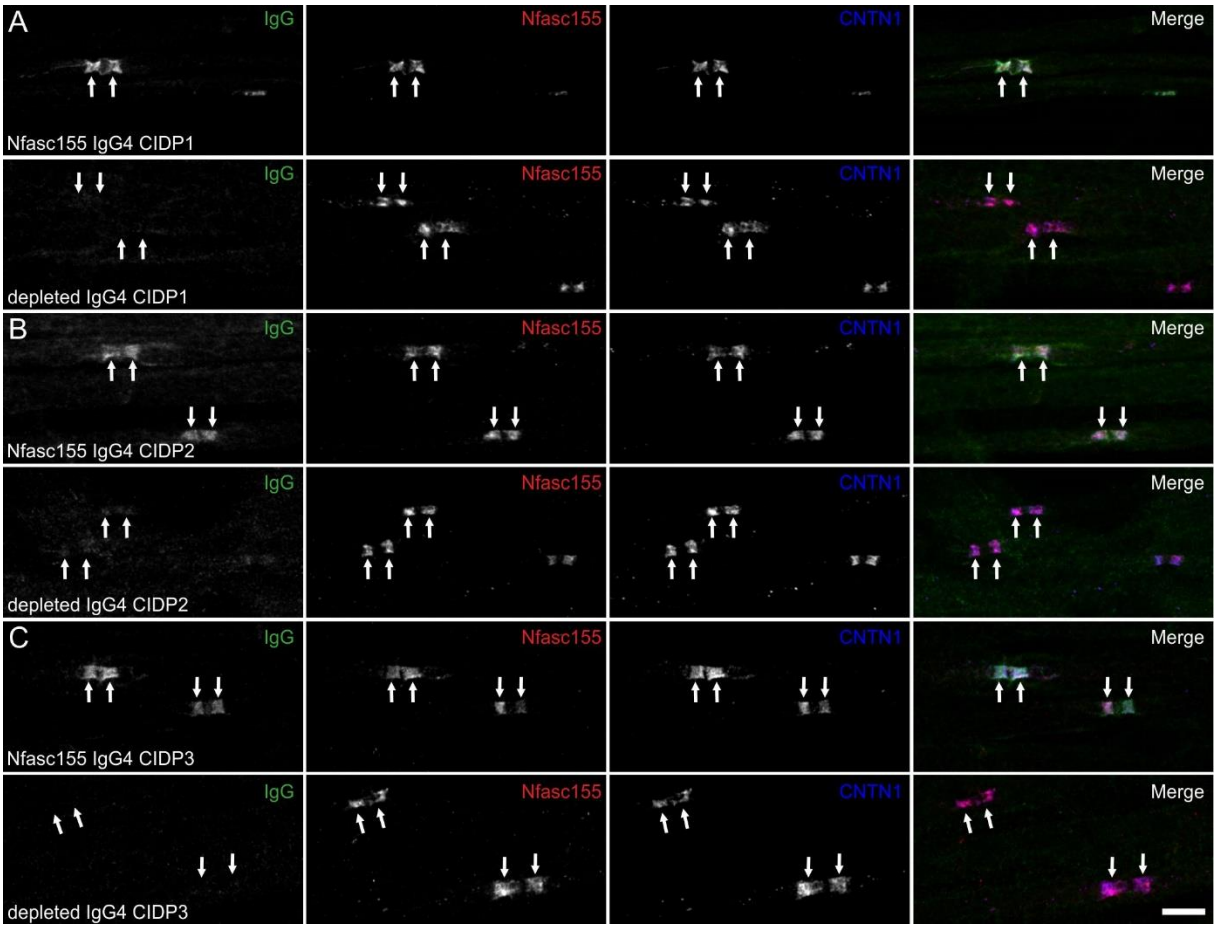

Supplemental Figure 4. Purified anti-Nfasc155 IgG4 react against Nfasc155 at paranodes.

(**A-C**) These are teased rat sciatic nerves immunostained for Nfasc155 (red), CNTN1 (blue) and the purified IgG4 fractions from three CIDP patients positive (CIDP1-3; green) before (upper panels) and after depletion of anti-Nfasc155 IgG4 (lower panels). The depletion of anti-Nfasc155 IgG4 abolished the reactivity toward paranodes confirming that autoantibodies specifically targets Nfasc155 at paranodes. Scale bar: 10 μm.

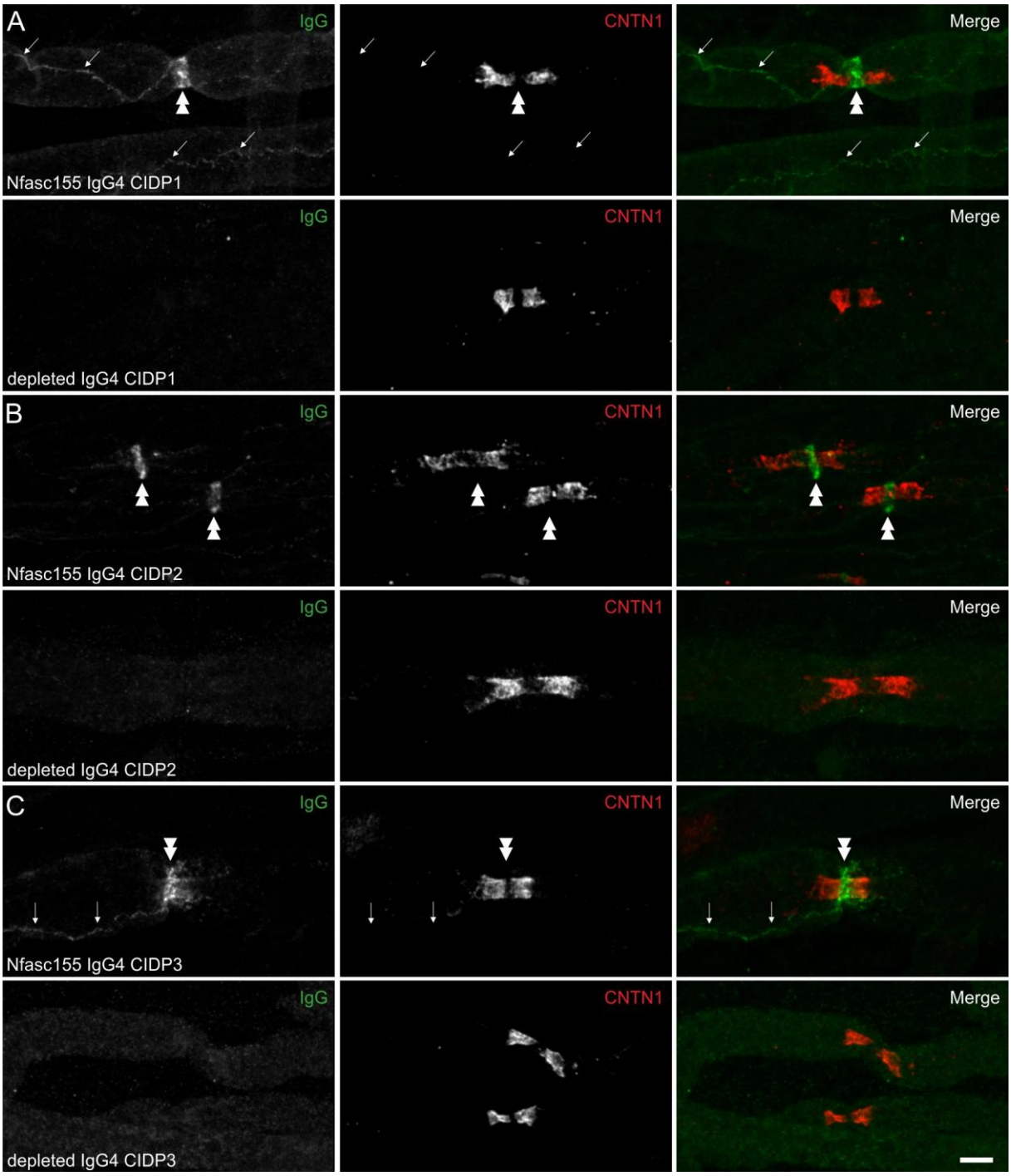

Supplemental Figure 5. Anti-Nfasc155 autoantibodies targets surface Nfasc155 on Schwann cells.

(**A-C**) Sciatic nerve fibers were incubated for 1 hour *in vitro* with purified IgG4 from CIDP patients (CIDP1-3; upper panels) or the IgG4 fraction depleted of anti-Nfasc155 IgG4 (lower panels). Nerves were fixed and immunolabeled for IgG4 (green) and CNTN1 (red). The depletion of anti-Nfasc155 IgG4 abolished autoantibodies binding at node vicinity (double arrowheads) and at adherens junctions along the internode (arrows). Scale bars: 10 μm.

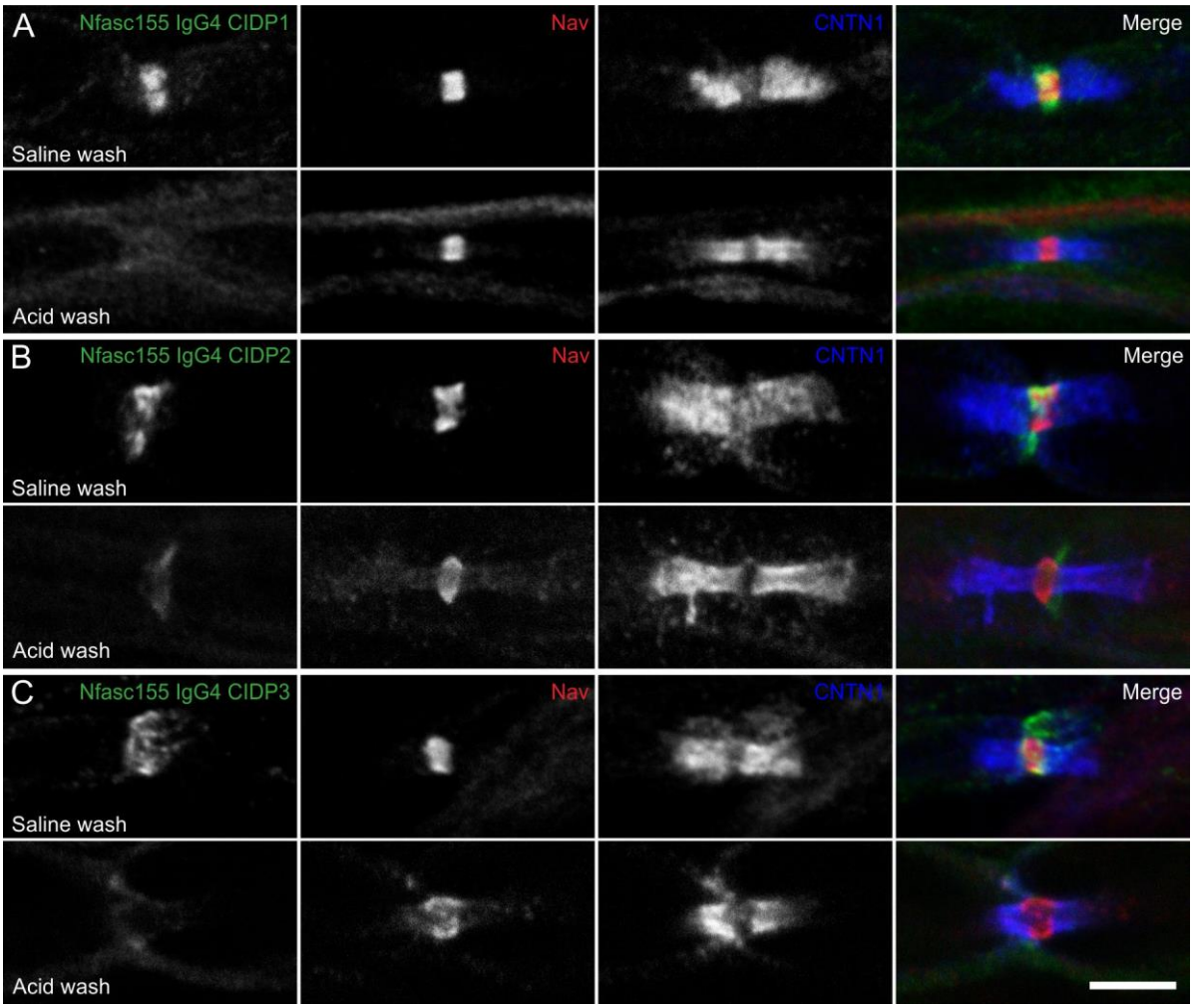

Supplemental Figure 6. Anti-Nfasc155 autoantibodies are not internalized from the Schwann cell surface.

(**A-C**) Sciatic nerve fibers were incubated for 1 hour *in vitro* with purified anti-Nfasc155 IgG4 from three CIDP patients (CIDP1-3). Nerve were then washed for 5 minutes with artificial CSF pH7.4 (upper panels) or pH2.0 (Acid wash; lower panels) to release surface bound antibodies. Nerves were fixed and immunolabeled for IgG4 (green), voltage-gated sodium channels (Nav; red), and CNTN1 (blue). Acid washes completely removed anti-Nfasc155 IgG4 immunostaining demonstrating that these antibodies were bound to Schwann cell surface and were not internalized. Scale bars: 10 μm.

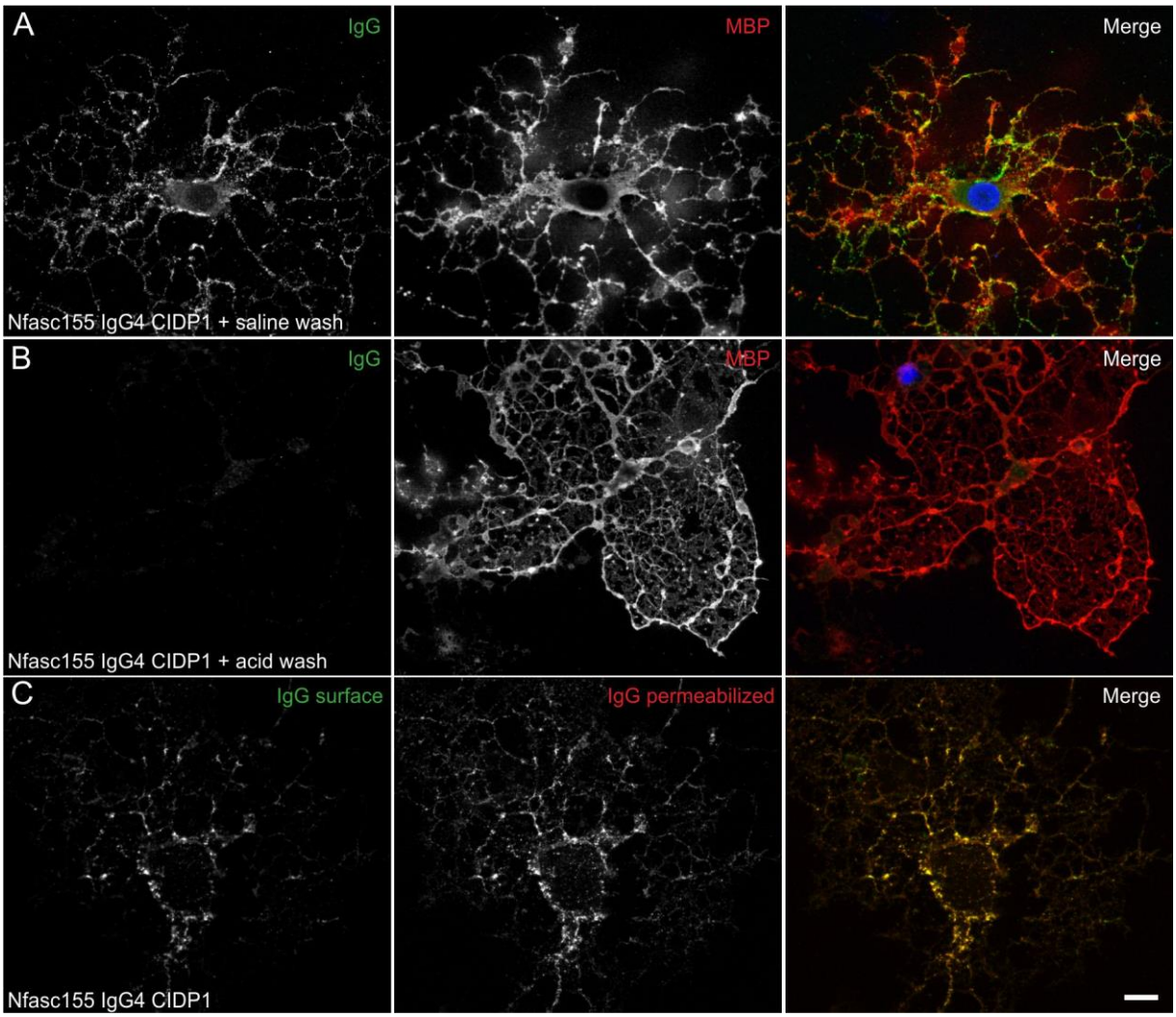

Supplemental Figure 7. Anti-Nfasc155 autoantibodies are not internalized from the oligodendrocyte surface.

(**A**-**B**) Oligodendrocytes (10 days *in vitro*) were incubated for 1 hour with anti-Nfasc155 IgG4 from patient CIDP1. Cells were then washed for 2 minutes with neurobasal medium pH7.4 (**A**) or pH2.0 (Acid wash; **B**). Cells were then fixed and immunolabeled for IgG4 (green) and myelin basic protein (MBP; red). Acid washes completely removed the surface bound anti-Nfasc155 IgG4. (**C**) Oligodendrocytes (10 days *in vitro*) were incubated for 1 hour with anti-Nfasc155 IgG4. Cells were washed, fixed and incubated with donkey anti-human IgG conjugated to Alexa 488. Then, cells were permeabilized and labeled with donkey anti-human IgG conjugated to Alexa 594. Surface (green) and total (red) IgG staining completely overlapped confirming that autoantibodies were not internalized. Scale bar: 10 μm.

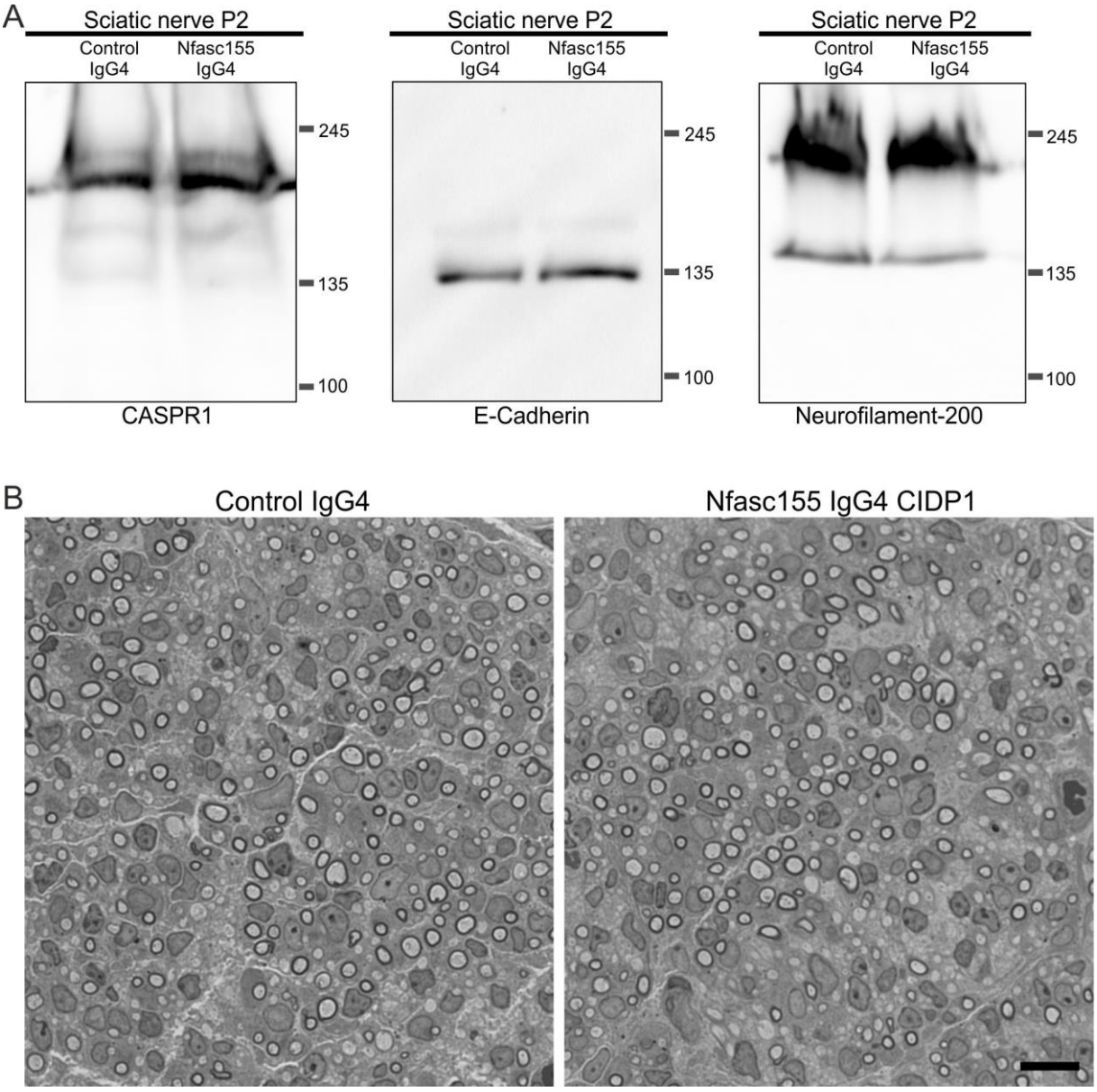

Supplemental Figure 8. Injection at P0 does not affect myelination.

(**A**) Sciatic nerve proteins (100 µg) from P2 animals injected with control IgG4 (n = 4) or anti-Nfasc155 IgG4 from patient CIDP1 (n = 4) at P0 were immunoblotted as indicated. The levels of or CASPR1, E-Cadherin, or Neurofilament-200 were not affected by anti-Nfasc155 IgG4. Molecular weight markers are shown on the right (in kDa). (**B**) These are representative pictures of transverse semi-thin sections of sciatic nerves from P2 animals injected with control IgG4 (left) or anti-Nfasc155 IgG4 (right) at P0. Myelination was not affected by the presence of anti-Nfasc155 IgG4. Scale bar: 10 µm.

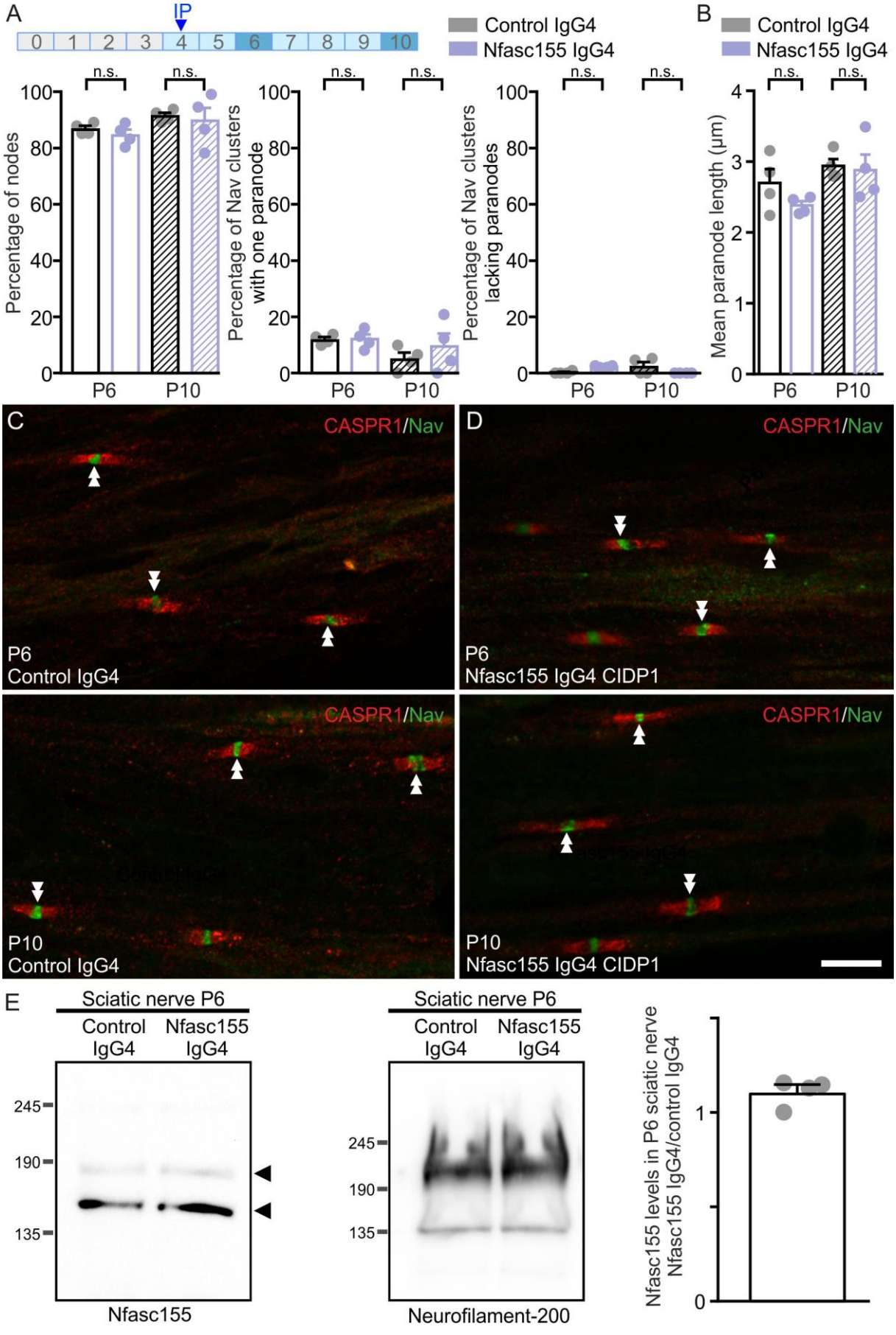

Supplemental Figure 9. Late injection of anti-Nfasc155 IgG4 at P4 does not affect

paranode stability.

(**A-D**) Rat pups received an intraperitoneal injection of 250 µg of control IgG4 or anti-Nfasc155 IgG4 from patient CIDP1 at P4 (n = 4 animals for each condition and age). Sciatic nerve fibers were immunolabeled for voltage-gated sodium channels (Nav; green) and CASPR1 (red) at P6 and P10. Paranodal length (**A**) and the percentage of Nav clusters with one or without CASPR1-positive paranodes and of nodes with two flanking CASPR-1 positive paranodes (**B**) were quantified at each age (n = 200-300 nodes or paranodes for each condition and age). Representative images are shown in **C** and **D**. At P6, the majority of Nav channel clusters were flanked by two CASPR1-positive paranodes. Injection of anti-Nfasc155 IgG4 did not affect paranodal length or the frequency of nodes with flanking paranodes. Scale bar: 10 µm. (**E-F**) Sciatic nerve (100 µg) from P6 animals injected with control IgG4 (n = 4) or anti-Nfasc155 IgG4 (n = 4) at P4 were immunoblotted with antibodies against Nfasc155 or neurofilament-200. Arrowheads indicate Nfasc155-H and Nfasc155-L isoforms. The levels of Nfasc155 were not affected in sciatic nerves of animals treated with anti-Nfasc155 IgG4 compared to control IgG4 (unpaired two-tailed Student's *t*-tests for two samples of equal variance). Molecular weight markers are shown on the left (in kDa). Bars represent mean and S.E.M.

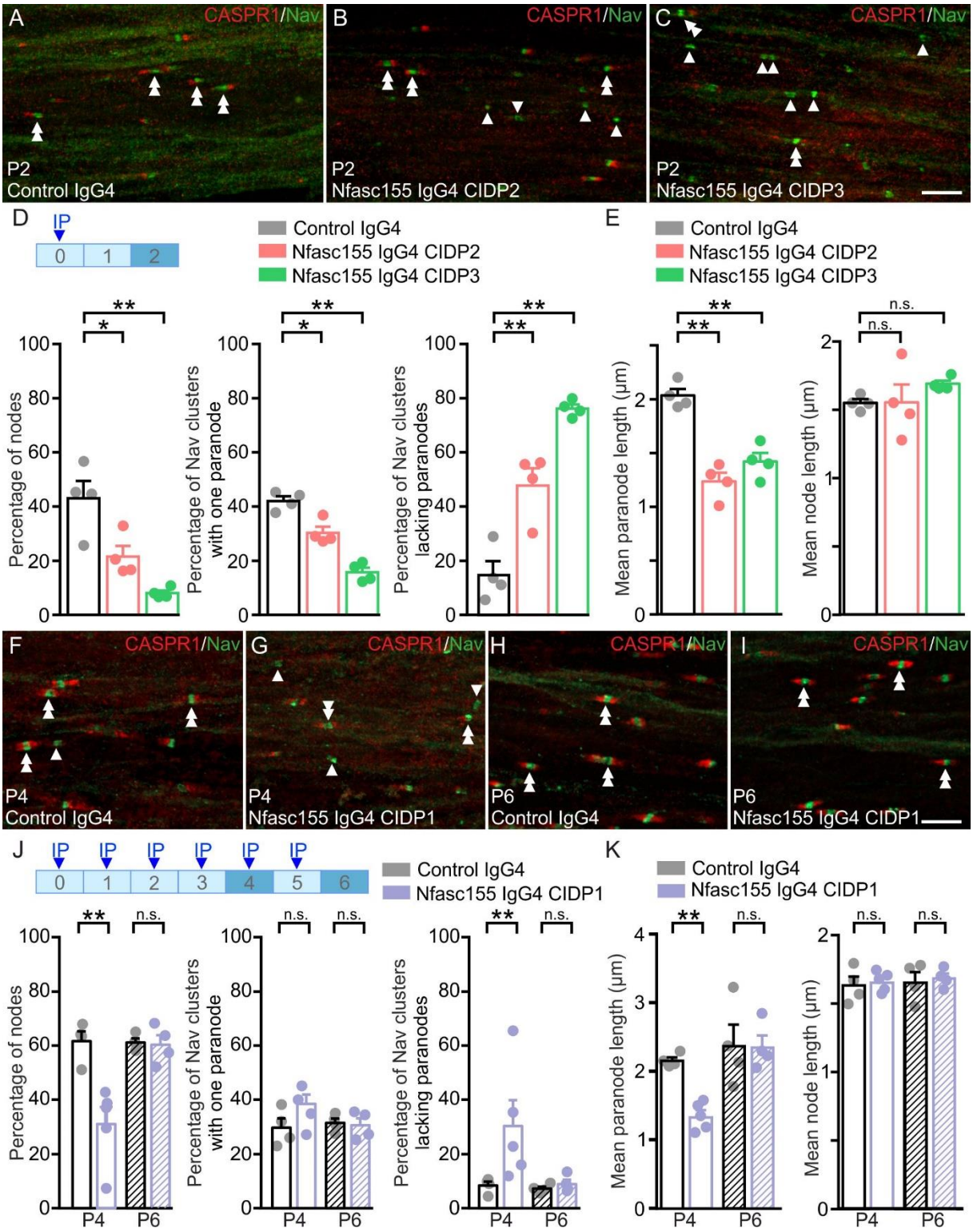

Supplemental Figure 10. The passive transfer of anti-Nfasc155 IgG4 affects paranode stability.

(**A-E**) New born rat pups received an intraperitoneal injection of 250 µg of control IgG4 (**A**) or anti-Nfasc155 IgG4 from patients CIDP2 (**B**) or CIDP3 (**C**) on the day of birth and were examined at P2 (n = 4 animals for each condition and age). Sciatic nerve fibers were fixed and immunolabeled for voltage-gated sodium channels (Nav; green) and CASPR1 (red). The

percentage of Nav clusters without CASPR1-positive paranodes (arrowheads) or with one CASPR1-positive paranodes, and of nodes with two flanking CASPR1-positive paranodes (double arrowheads) were quantified at P2 (**D**), as well as the paranodal and nodal (**E**) lengths (n = 200-300 nodes or paranodes for each condition and age). Injection of anti-Nfasc155 IgG4 from both patients importantly delayed the formation of CASPR1-positive paranodes. As for anti-Nfasc155 IgG4 from CIDP1, a significantly higher percentage of hemi-nodes without flanking paranodes was observed at P2 in animals receiving anti-Nfasc155 IgG4 from patients CIDP2 and CIDP3 (* $P<0.05$; ** $P<0.005$ by one-way ANOVA followed by Bonferroni's post-hoc tests). Paranodal length was also significantly shorter in these animals (** $P<0.005$ by one-way ANOVA followed by Bonferroni's post-hoc tests) however, the nodal length was not affected. (**F-K**) New born rat pups received a daily intraperitoneal injection of 250 µg of control IgG4 (**F**) or anti-Nfasc155 IgG4 from patient CIDP1 from the day of birth to P6, and animals were examined at P4 and P6 (n = 4-5 animals for each condition and age). Sciatic nerve fibers were labeled for voltage-gated sodium channels (Nav; green) and CASPR1 (red), and paranode formation was quantified at P4 and P6 (**J**), as well as the paranodal and nodal (**K**) lengths. The prolonged administration of anti-Nfasc155 IgG4 was associated with a significant decrease in CASPR1-positive paranodes at P4, but not at P6 (** $P<0.005$ by one-way ANOVA followed by Bonferroni's post-hoc tests). Paranodal length was also significantly shorter at P4 (** $P<0.005$ by one-way ANOVA followed by Bonferroni's post-hoc tests), but was not affected at P6. Nodal length was not affected at both ages. Bars represent mean and S.E.M. Scale bar: 10 µm.

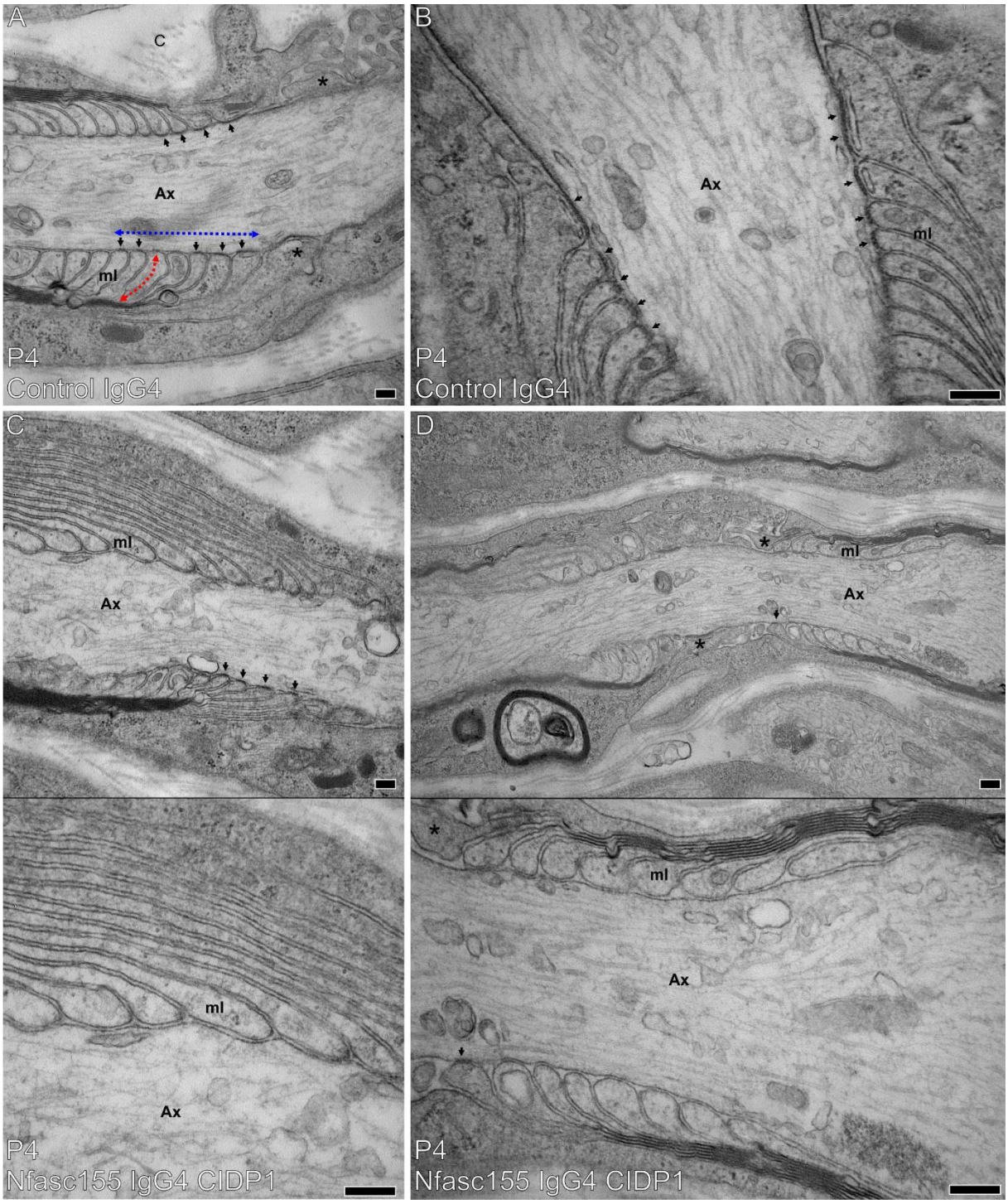
A
C
*
Ax
ml
*
P4
Control IgG4
B
Ax
ml
P4
Control IgG4
C
ml
Ax
ml
Ax
P4
Nfasc155 IgG4 CIDP1
D
*
ml
Ax
*
*
ml
Ax
P4
Nfasc155 IgG4 CIDP1

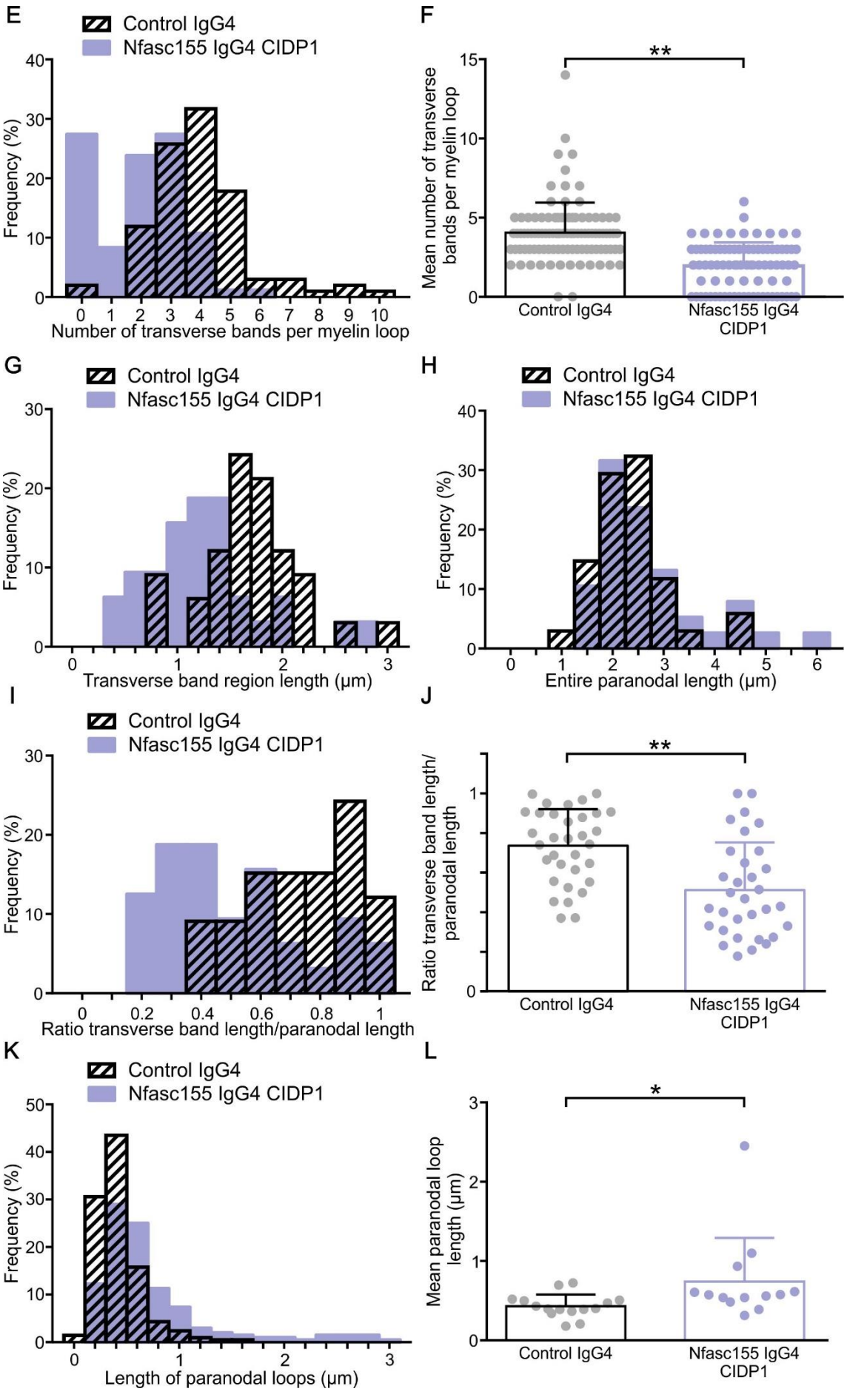
E
Control IgG4
Nfasc155 IgG4 CIDP1
Frequency (%)
Number of transverse bands per myelin loop
F
**
Mean number of transverse bands per myelin loop
Control IgG4
Nfasc155 IgG4 CIDP1
G
Control IgG4
Nfasc155 IgG4 CIDP1
Frequency (%)
Transverse band region length (μm)
H
Control IgG4
Nfasc155 IgG4 CIDP1
Frequency (%)
Entire paranodal length (μm)
I
Control IgG4
Nfasc155 IgG4 CIDP1
Frequency (%)
Ratio transverse band length/paranodal length
J
**
Ratio transverse band length/ paranodal length
Control IgG4
Nfasc155 IgG4 CIDP1
K
Control IgG4
Nfasc155 IgG4 CIDP1
Frequency (%)
Length of paranodal loops (μm)
L
*
Mean paranodal loop length (μm)
Control IgG4
Nfasc155 IgG4 CIDP1

Supplemental Figure 11. Electron microscopic alterations at paranodal regions in animals treated with anti-Nfasc155 IgG4.

(**A-D**) Electron microscopic examination of longitudinal sections of sciatic nerves from P4 rats treated with control IgG4 (**A-B**) or anti-Nfasc155 IgG4 from patient CIDP1 (**C-D**) from P0 to P4. At P4, many mature nodes of Ranvier were observed. In control animals, numerous septate-like junctions (arrows) were observed at paranodal regions, notably at the vicinity of the node of Ranvier. Two representative nodes are shown in **A** and **B**. In animals treated with anti-Nfasc155 IgG, paranodal regions were mostly devoid of septate-like junctions or presented a strong decrease in the number of septate-like junctions. In some cases (**C**), septate-like junctions were observed at the vicinity of the node (upper panel), but not in paranodal myelin loops distant from the node (the lower panel shows a higher magnification of the same paranode). In other, septate-like junctions were completely absent from paranodes (the lower panel shows a higher magnification of the same paranode). No alterations of the microvilli that covered the nodal gap (asterisk) were observed. Ax: axon; C: collagen; ml: myelin loops. Scale bars: 200 nm. (**E-F**) The number of transverse bands per paranodal myelin loops was quantified in high magnification pictures of 16-17 nodes of Ranvier from control animals or from animals treated with anti-Nfasc155 IgG4. Only the five paranodal loops bordering the nodes of Ranvier were used for quantification. A significantly lower number of transverse bands were observed in anti-Nfasc155 IgG4 treated animals (** $P<0.005$ by unpaired Student's *t*-test and Kolmogorov-Smirnov test). (**G-L**) The length of paranodal regions containing transverse bands (**G**; blue dashed lines in **A**), of the entire paranodal region (**H**), and of paranodal loops (**K-L**; red dashed lines in **A**) were measured in 32-33 paranodes from control animals or from animals treated anti-Nfasc155 IgG4. The ratio of tranverse band-containing regions to the entire paranodal length was then calculated (**I-J**). Albeit the length of the entire paranodal region was not significantly different between control and treated animals (**H**), the regions that contained

transverse bands (blue dashed lines in **A**) were significantly shorter in animals treated with anti-Nfasc155 IgG4 (**G**; $P<0.005$ by unpaired Student's *t*-test and Kolmogorov-Smirnov test). This indicated that anti-Nfasc155 IgG4 did not affect myelination or paranode formation but deteriorated transverse band formation. In addition, paranodal loops appeared modestly lengthened in anti-Nfasc155 IgG4 treated animals (**K-L**; $P<0.05$ by unpaired Student's *t*-test and Kolmogorov-Smirnov test), suggesting that anti-Nfasc155 IgG4 may impact myelin compaction in paranodal loops at this age. Bars represent mean and S.D.

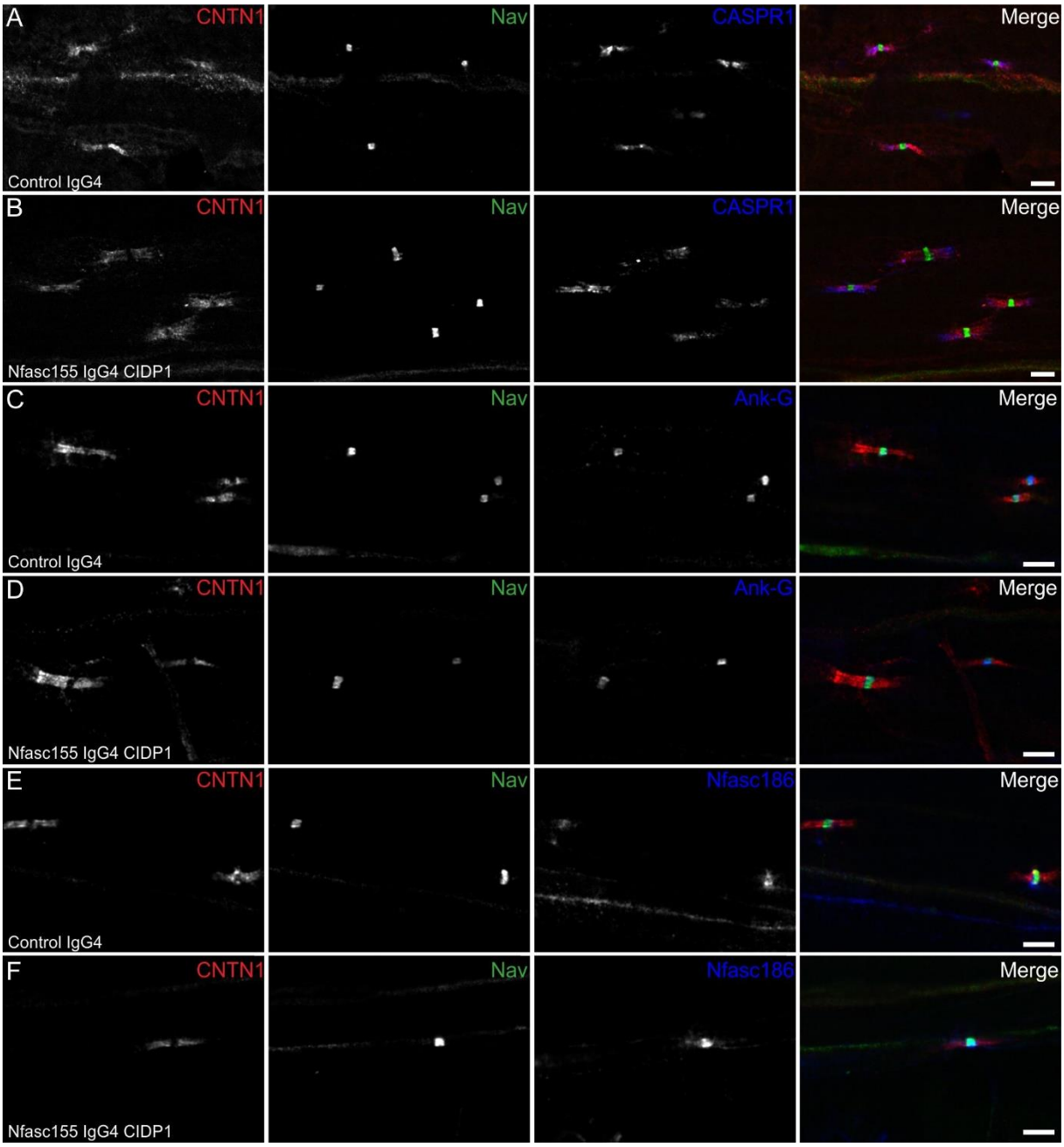

Supplemental Figure 12. Anti-Nfasc155 IgG4 does not alter the paranodal specialization of dorsal spinal nerve.

(**A**-**F**) Teased fibers from L6 dorsal roots of animals treated with control IgG4 (n = 15; **A**, **C**, and **E**) or anti-Nfasc155 IgG4 from patient CIDP1 (n = 15; **B**, **D** and **F**) were stained for Nav channels (green), CNTN1 (red) and CASPR1 (blue; **A**-**B**), ankyrin-G (Ank-G; blue, **C**-**D**), or Nfasc186 (blue, **E**-**F**). In both animals injected with control IgG4 or anti-Nfasc155 IgG4, the majority of the nodes of Ranvier were positive for Nav channels, ankyrin-G and Nfasc186 clusters and were bordered by CASPR1 and CNTN1-positive paranodes. Scale bars: 10 μm.

Supplemental video: Clinical phenotype of animals treated with anti-Nfasc155 IgG4.

These are representative videos showing tail spasticity and gait abnormalities in an animal treated with anti-Nfasc155 IgG4 from patient CIDP1 and the normal gait of a control animal.